Mineral physical protection and carbon stabilization in-situ evidence revealed by nano scale 3-D tomography

Yi-Tse Weng[1,#], Chun-Chieh Wang[2,#], Cheng-Cheng Chiang[2],Heng Tsai[3], Yen-Fang Song[2], Shiuh-Tsuen Huang[4], Biqing Liang[1,*]

[1]National Cheng Kung University, Department of Earth Sciences, Tainan, Taiwan ROC

[2]National Synchrotron Resource Research Center, Hsinchu, Taiwan ROC

[3]National Changhua University of Education, Department of Geography, Changhua, Taiwan ROC

[4]National Taichung University of Education, Department of Science Education and Application, Taichung, Taiwan ROC

[#]Equal Contribution

[*]Corresponding author: Biqing Liang
(liangglobalcarbon@gmail.com;liangbq@mail.ncku.edu.tw)

Abstract

An approach for nano scale 3-D tomography of organic carbon (OC) and associated mineral nano particles was developed to illustrate their spatial distribution and boundary interplay, using synchrotron-based transmission X-ray microscopy (TXM). The proposed 3-D tomography technique was first applied to in-situ observation of a lab-made consortium of black carbon (BC) and nano mineral (TiO_2, 15 nm), and its performance was evaluated under dual-scan absorption contrast and phase contrast modes. Then this novel tool was successfully applied to a natural OC-mineral consortium from high mountain soil at a spatial resolution down to 60 nm, showing the fine structure and boundary of OC, distribution of abundant minerals at nano size, and in-situ 3-D organo-mineral association. The stabilization of aged natural OC was found attributed to the

physical protection of SRO/Fe-containing minerals (Fe oxyhydroxides including ferrihydrite, goethite, and lepidocrocite) of nano size, and the strong organo-mineral complexation. The sorption of OC (and cation) to Fe oxyhydroxides through organo-mineral multiple complex bonds ~~such as 'ligand exchange'~~ could occupy and consume their respective reactive surface sites, tune down their activity and enhance their respective stabilization. The ubiquitousness and abundance of mineral nano particles, and their high heterogeneity in natural environment could have been seriously underestimated by traditional study approach. Our in-situ description of organo-mineral interplay at nano scale provides direct evidence to substantiate the importance of mineral physical protection for OC long term stabilization. ~~Mineral physical protection for OC stabilization may be more important than previous understanding.~~ This high resolution 3-D tomography tool is promising for new insight on the interior 3-D structure of micro-aggregates, in-situ organo-mineral interplay, and the fate of mineral nano particles including heavy metals in natural environment.

Introduction

Mineral association with organic carbon (OC) may be an important stabilization mechanism for carbon long-term sequestration, yet little is known about their in-situ interplay and extent of association on aggregation level either chemically or physically (Baldock and Skjemstad, 2000; Cusack et al., 2012; Mikutta et al., 2006; Torn et al., 1997;

Vogel et al., 2014). Traditional fractionation methods based on size and external force for dissecting the association strength between OC and minerals in soils are limited to bulk sample. High resolution information and in-situ knowledge is required for interpretation of fractionation results and modeling (Kaiser et al., 2002; Kleber et al., 2007; Sollins et al., 2009). Nano scale two-dimensional isotopic mapping discovered that only a limited amount of the clay-sized surfaces contributed to OC sequestration (Vogel et al., 2014). Understanding OC interplay with minerals in the fine fraction warrants study in a three dimensional way (Kinyangi et al., 2006; Lehmann et al., 2007; Lehmann et al., 2008; Solomon et al., 2012). Detailed in-situ association information between OC and minerals may lead to breakthrough on mineral physical protection mechanism for OC long term stabilization. To overcome the limitations of commonly used electron microscopic methods (such as only on the surface layer, and undesirable artifacts due to pretreatments), non-destructive high-resolution X-ray 3-D tomographic technique will be used for exploring the fine structure of OC and boundary interplay with mineral nano particles.

High resolution Synchrotron-based TXM has been demonstrated as a powerful tool for understanding the internal 3-D structure of particles down to nano meter scale, due to its large penetration depth and superior spatial resolution (Kuo et al., 2011; Wang et al., 2015). This technique was successfully applied to reveal the discrete three dimensional micro-aggregation structure of clay (kaolinite) in natural aqueous environment, and generated remarkable tomography that revealed precise inter-particle structure (Zbik et al., 2008) as well. Clay particles with diameter below 500 nm were

clearly visible and their pseudohexagonal symmetry was recognized in details in a three dimensional way.

The synchrotron-based TXM at the beamline BL01B1 of Taiwan Light Source (TLS), which has been used in this study, provides two-dimensional imaging and three-dimensional tomography at a spatial resolution of 30/60-nm with tunable energy (8-11keV). It provides unprecedented opportunity for studying OC boundary interplays with mineral particles at nano meter scale. Two image acquisition modes, absorption contrast and phase contrast, can be used alternatively for recognizing OC and nano minerals. Conventionally, X-ray images are taken in the absorption contrast mode, and the resulting image contrast only depends on the difference of X-ray attenuation coefficient between materials. This mode is especially useful for materials consisted of high atomic number compositions. However, in organic materials, the difference of X-ray attenuation coefficients between specimen and air is too small to distinguish each other. For this reason, the structure of organic materials is often hard to be recognized due to low contrast in absorption contrast images. Alternatively, phase contrast technique transfers optical path length differences (optical phase) inside specimens into intensity contrast, can be used for imaging low atomic number materials, which are poor to absorb X-rays. It provides a unique opportunity to observe fine structures of organic specimens such as OC. Little study has been done on OC and mineral nano particles using high-resolution 3-D X-ray tomography, though non-synchrotron-based 3-D X-ray microscopy was used to observe occluded carbon in phytolith structure and kerogen in micrometer scale (Alexandre et al., 2015; Bousige et al., 2016). We aim to develop a new dual-scan method

using phase contrast and absorption contrast modes of the TXM alternatively for the observation of OC and mineral consortiums inside lab-made and natural samples in nano meter scale. Lab-made OC in forms of black carbon (BC) will be examined in the artificial consortium with added nano mineral (TiO_2) particles using synchrotron-based TXM for the first time.

Black C/biochar has received increasing research interest globally due to its importance in global carbon cycling, soil fertility improvement and environmental pollutant remediation (Bond et al., 2013; Jeffery et al., 2015; Kuhlbusch, 1998; Lehmann et al., 2007; Liang et al., 2006; Liang et al., 2008; Schmidt, 2004). On top of method development for 3-D tomography at nano meter scale, this study provides in-situ evidences on the minerals physical protection on natural OC, and to explore the C stabilization mechanism in natural soil.

Methodology

Sample preparation and background

Black C was made in lab using leguminous plant (*Sesbania roxburghii*) of 80 days' harvest, which was first oven-dried (65 ℃) and charred inside a muffle furnace at 300 ℃ in loosely sealed stainless containers (Chen et al., 2014b). This consortium of low temperature BC and mineral nano particles was constructed by dry deposition of commercial TiO_2 (15 nm) on lab-made BC (3 mm chunk), and then embedded in Gatan G-1 epoxy. The block were cross sectioned to a thickness of 100 to 200 μm using a

microtome (Leica Reichert Ultracut E ultra-microtome) and subsequently hand-polished to a thickness of 30 to 50 μm. Each section was transferred onto Kapton tape and mounted on a stainless steel sample holder for TXM observation. Before TXM analysis, gold nano particles (50-150 nm or 400-500 nm in diameter) were deployed on the section surface for image registration before 3-D tomography reconstruction.

Thin section of natural OC and mineral consortium (NH) was prepared using micron to millimeter size particulate sample from high mountain soil. Particulate organic matter of mm-size with minerals embedded inside was taken from the lower dark layer at depth of 72-93 cm in a Typic Humicryepts soil profile, located in Mt. Nanhua, Nantou County, Taiwan (24°03'00", 121°17'02"). On top of this dark layer, iron stain was observed within the depth of 63-72 cm in the profile. The soil has developed on top of sandstone and slate, with some features of inceptisol and spodosol. The sampling elevation is 3092 m, the annual temperature is 7.57 °C, and the yearly rainfall is 2203.1 mm. The major vegetation is arrow bamboo (*Yushania nittakayamensis*), with sporadic Hemlock (*Tsuga chinensis*), fir (*Abies kawakamii*), and spruce (*Picea morrisonicola*).

The sequestration environment represents weak leaching and inactive chemical weathering conditions. The age of soil organic C has been estimated to 3500 years B.P.

Working conditions of TXM

A superconducting wavelength shifter source provides a photon flux of 4×10^{11} photons s^{-1} (0.1% bw)$^{-1}$ in the energy range of 5-20 KeV at the BL01B1 beamline. A

1 double crystal monochromator exploiting a pair of Ge (111) crystals selects X-rays within

2 the energy range of 8-11 KeV. The specimen is imaged using a Fresnel zone plate, which

3 is used as an objective lens for an image magnification of 44× by the first order diffraction

4 mode. Conjugated with a 20× downstream optical magnification, the TXM provides a total

5 magnification of 880× with a field of view of 15×15 μm^2. By acquiring a series of 2D

6 images with the sample rotated 1º stepwise, 3-D tomography datasets is later

7 reconstructed based on 151 sequential image frames that are captured with azimuth

8 angle rotating from -75º to +75º.

9

10 **Image acquisition for 3-D tomography**

11 Under the most frequently used absorption contrast mode, 2-D images are

12 recorded based on the projection of the different X-ray absorption coefficient integration

13 along the optical pathway through samples on a detector. The absorption mode is useful

14 for materials of high absorption coefficient, such as minerals or high atomic number

15 materials, but it is poor for the observation of low atomic number materials, such as

16 organic or polymer materials. In order to recognize the OC structure more accurately, 2-

17 D/3-D images for the same sample region are recorded using absorption contrast and

18 phase contrast modes, respectively.

19 In the phase contrast mode, the gold-made phase ring positioned at the back-focal

20 plane of the zone plate is used to retard or advance the phase of the non-diffractive light

by π/2, generating (Zernike's) phase contrast images recording at the detector. The light diffracted by specimen is interfered with the retarded non-diffractive light, generating phase contrast image. The intensity difference in a phase contrast image shows the combination of optical phase difference and absorption difference through specimens. This ability is especially important for the observation of OC which has a low X-ray absorption coefficient.

3-D reconstruction and analysis

Three dimensional tomography reconstruction is performed using homemade software, which is coded based on iterative image registration (Faproma) (Wang et al. 2017) and filtered back projection (FBP) reconstruction algorithms. Firstly, a serial of single TXM image captured from -75⁰ to +75⁰ at rotational increments of 1° is loaded to do image registration automatically using Faproma algorithm. Finally, the reconstruction is processed using FBP algorithm. The reconstructed dataset is exported in cross-sections, and later used for 3-D visualization using *Amira*. The intensity contrast of reconstructed datasets is inversed for better visualization; Compositions with higher absorption coefficients are shown in higher intensity and with low absorption coefficients are shown in lower intensity. The exported cross-section of 3-D tomography (reconstructed datasets) shows the real distribution details and boundary interplay of OC and mineral particles. The final 3-D tomographic structures for visualization and illustration are generated using *Amira* 3-D software for image post-process and computation (Fig. S1).

1

Elemental mapping by SEM-EDS

3   For correlated spatial distribution of selected elements (C, O, Fe, Al) in natural OC

4 particles from high mountain soil, a low-vacuum scanning electron microscope (JEOL W-

5 LVSEM, JSM-6360LV) equipped with an energy dispersive X-ray spectrometer (Oxford

6 EDS) and a cathodoluminescence (CL) image detector (Gatan mini-CL) was used for

7 elemental mapping, at an accelerating voltage of 15 KeV.

8

X-ray Diffraction for Mineralogy

10   To analyze the forms of minerals associated with natural OC, particulate OC (with

11 minerals on surface and embedded inside) was grounded and injected into capillary tubes

12 (Special Glass 10, Hampton Research, CA) for synchrotron high resolution X-ray

13 diffraction analysis at 09A beamline at Taiwan Photon Source (TPS), which is equipped

14 with a set of high-resolution monochromator (HRM). The wavelength is 0.8266 Å at the

15 energy of 15 KeV. The XRD spectra were recorded under room temperature for 240s

16 accumulation time and specific X-ray diffraction peaks and patterns were assigned ICDD

17 using PDF-2/4 program.

18

Carbon functionality and interfacial mineral forms using SR-FTIR

20   For FTIR analysis, mineral-bearing OC (NH) particles were grounded, dried (60 ℃

21 overnight), and mixed with potassium bromide (KBr) at a ratio of 1:100, and molded into

disks using a hydraulic press. During the pressing process, a vacuum pump was used for evacuating air and water. The samples were measured using Infrared Microspectroscopy (IMS) at the BL14A1 beamline of the National Synchrotron Radiation Research Center (NSRRC), Taiwan. The FTIR spectra were collected up to 1024 scans in the mid-infrared range of 4000-400 cm^{-1} with a spectral resolution of 4 cm^{-1}, using a FTIR spectrometer (Nicolet 6700, Thermo Fisher Scientific, Madison, WI, USA) with a self-equipped light source. The automatic atmospheric suppression function in OMNIC (OMNIC 9.2, 2012; Thermo Fisher Scientific Inc., Waltham, MA, USA) for bulk sample analysis was activated for data analysis, to eliminate the rovibration absorptions of CO_2 and water vapor in ambient air.

Results and Discussions

Distinguish the fine structure of BC and boundary interplay with mineral nano particles

High resolution 2-D X-ray photographs were captured for the identical regions in lab-made BC and nano mineral consortium using dual-scan absorption contrast and phase contrast modes (Fig. 1, a, e). The cross-section views exported from the reconstructed 3-D datasets reveal subtle details of BC and mineral nano particles, and clearly outline the fine boundary of BC and the distribution of TiO_2 nano particles (Fig. 1). The shape, size, and distribution of mineral nano particles can be identified accurately using absorption contrast mode due to their high X-ray absorptivity (Fig.1, b, c and d). In comparison, the BC structure and contour of its boundary can be revealed much more

clearly using phase contrast mode (Fig.1, f, g and h). However, the bright halo artifacts in phase-contrast image enhance the intensity of margin texture for nano minerals, and may lead to overestimation of their volume (Fig. 1, e, f, g and h). Use of dual-scan mode allows cross-checking of details and validation.

Cross-section views of the reconstructed 3-D tomography share consistent and comparable features of BC and nano minerals in multi-angles (Fig. 2). According to the display of different slicing planes (XY, XZ, YZ), it can be recognized that TiO_2 nano particles deposit inside BC only sporadically contact with BC boundary (Fig. 2, b, e, c, and f) due to the treatment of dry deposition. The nano scale gap between BC and nano minerals has been clearly observed in absorption and phase-contrast images (Fig. 2, b, e, c, and f). It is feasible to calculate the interplay surface and mineral volume quantitatively by examining each cross-section views in a selected region. Our approach is a success in thorough exploration of OC and minerals 3-D distribution, and verification of their real in-situ spatial correlation under nano scale resolution.

3-D tomography for illustrating in-situ distribution of BC and mineral nano particles

3-D tomography for visualization has been computed and generated to illustrate the spatial correlation between BC and minerals based on post-process of reconstructed 3-D datasets. Unprecedented details of 3-D in-situ distribution of BC and mineral nano particles are revealed in computed 3-D tomography (Fig. 3; Fig. SMOV1, 2). Results from absorption mode and phase contrast mode are consistent and comparable. The fine

boundary feature of BC is contoured to a more completeness in the phase contrast mode. The OC was rendered by transparent mode and high absorptivity materials (such as minerals and gold particles) were rendered by solid mode with various colors. All renderings are combined to visualize their interaction. The illustration of 3-D computed tomography allows randomly tilted and set angles for image and animated video exports, thus any region of interest inside a specimen may be explored thoroughly.

The lab-made consortium was successfully tested by this dual-scan methodology using both absorption contrast and phase-contrast acquisition modes (Figs. 1, 2, 3). Low temperature BC, which is more similar to natural OC (especially recalcitrant OC) than that made at high temperature, was especially made to test its applicability under absorption contrast mode. Results show that the fine structure and boundary of low temperature BC can be clearly observed under absorption contrast mode. Thus for environmental OC samples, the use of absorption contrast mode is probably sufficient for capturing organo-mineral features.

Different from field samples, the minerals observed within the lab-made consortium often distribute in clusters and are only sparsely in association with BC surface. The preservation of plant-like structures in BC could play a role for carbon stabilization in natural environment, as their porosity and reactive surface provide large areas and sites for mineral coating, which may contribute to their long residence and physical endurance (Eusterhues et al., 2008; Rasmussen et al., 2005; Rawal et al., 2016).

Interplay of OC and minerals and C stabilization in high mountain soil

Nano scale 3-D tomography revealed a high heterogeneity within OC-mineral consortium and most particulate OC surface is coated by minerals. ~~provides new insight for the mineral physical protection mechanism of OC in soil.~~ Natural OC exhibited strong organo-mineral association on its surface at nano scale in high mountain soil (Fig. 4; Fig. SMOV3). Abundant short-range order minerals in forms of subhedral particle or anhedral nano-aggregate have direct association~~contact~~ with the boundary of OC, and develop coating on the tracheid surface (Fig. 4 b and c) (Mikutta et al., 2006). Sheet-like mineral coating is observed on OC surface, which are dense and thin layers, likely originated from absorption. Another distinct texture is recognized as nano-aggregates/clusters of various shapes, possibly formed by OC-mineral co-precipitation. Mineral aggregation by poorly crystalline nano particles renders natural sub-micron porosity, which may contribute to elevated sorption capacity in soil (Rawal et al., 2016). The densely-packed mineral texture suggested significant physical protection on OC surface (Kaiser and Guggenberger, 2007). The sorbed minerals not only can form physical protection, but also could shield OC from chemical weathering (Mikutta et al., 2006). The key working minerals for OC-mineral interplay are essentially nano particles/submicron/SRO/poorly crystalline minerals.

The nature of associated minerals was confirmed to be mainly SRO Fe oxyhydroxides, specifically ferrihydrite (ICDD 01-073-8408), goethite (ICDD 01-073-6522), lepidocrocite (ICDD 00-044-1415), and quartz (ICDD 00-033-1161) (Fig. 5; Table S1), analyzed using high resolution synchrotron-based XRD. Quartz may be at most a

minor component on OC surface, considering their chemistry and particle size. Yet siliceous mineral surfaces may become coated with a veneer of hydrous Al- and Fe-oxides, which could confer net positive charge and promote their reactivity in tropical environments (Chen et al., 2014a; Sposito, 1989).

Considering their high surface area and reactivity, the abundant nano scale Fe oxyhydroxides could play a significant role for OC long-term stabilization through chemical bonding and physical shielding (Eusterhues et al., 2005; Kaiser et al., 2002; Kiem and Kogel-Knabner, 2002; Mikutta et al., 2006), as well as cation sorption in soil, and contribute to longevity of OC in high mountain soil. According to elemental mapping results, aluminosilicates may also be present, however, their portion and crystalline level should be low due to their minimal signal in the XRD spectra (Figs. 5, 6). The FTIR analyses reveal the chemistry of organo-mineral association (Fig. 7; Table S2). The aged OC is highly aromatic when at the same time highly reactive, as broad bands centered at 1596 cm^{-1} and 1706 cm^{-1} for aromatic C=C stretching and ν C=O in carboxyl are observed , pointing to likely origin of pyrogenic C (Özçimen and Ersoy-Meriçboyu, 2010; Sharma et al., 2004). Both aromatic and carboxyl C functional groups normally have high affinity with Fe (III) (Mikutta et al., 2007; Zhao et al., 2016). The broad bands point to possible significant degree of association between OC and minerals (Chen et al., 2016; Gu et al., 1994; Kaiser and Guggenberger, 2007). The sorption of OC to Fe oxyhydroxides through organo-mineral multiple complex bonds such as 'ligand exchange' could occupy and consume the reactive surface sites on OC and Fe oxyhydroxides, tune down their activity and enhance their respective stabilization (Chorover and Amistadi, 2001; Cornell

14

and Schwertmann, 2006; Hall et al., 2016; Kaiser and Guggenberger, 2007; Mikutta et al., 2007). The discovery of short-range-order mineral ferrihydrite in air-dried OC particles and later ground samples indirectly validates its stabilization due to organo-mineral interplay. As a SRO/metastable mineral, ferrihydrite is hard to estimate accurately in dry soil samples due to its transient nature and the limitation of traditional extraction and spectroscopic methods (Cornell and Schwertmann, 2006). The specific mineral forms phase in direct contact with OC on surface at nano scale warrants future study (Fig. SMOV3). In-situ mineral mapping of different SRO minerals/–Fe oxyhydroxide on OC surface will provide mechanistic evidence on OC stabilization. Mineral physical protection on OC may represent the end stage of carbon stabilization, especially in a weak leaching and weathering environment.

Our in-situ description of organo-mineral interplay at nano scale provides direct evidence on the important role of mineral physical protection for OC long term stabilization. High amounts of ferrihydrite and other Fe oxyhydroxides were also found associated with lignin-like OC in soil under an aquic moisture regime (Eusterhues et al., 2011). The abundance of mineral nano particles, and their high heterogeneity and short-range-order nature could be common in humid environment, however, they could have been seriously underestimated by traditional analysis methods, such as electron microscopy/X-ray diffraction/fractionation approaches, which focus on clay-size minerals (Mikutta et al., 2005). Mineral physical protection for OC stabilization may be more important than previous understanding. More research is proposed to explore: i) whether it is a general phenomenon that the minerals interact with OC are essentially nano

particle/submicron/SRO/poorly crystalline minerals, ii) whether the major mineral for C stabilization is nano scale SRO instead of clay-size mineral in soils. Perspective on C stabilization and saturation should take account the role of SRO minerals into soil C dynamics modelling, besides clay type and content.

In summary, a high resolution 3-D tomography tool is required for exploring the in-situ interplay of OC and nano minerals in natural environment. Nano scale 3-D tomography provides direct evidence and new insight for the mineral physical protection mechanism of OC in soil. This high resolution 3-D tomography approach is a promising technique for probing the multi interfacial features between OC and minerals in lab and field samples, and may provide new perspective on the fate of nano particles including heavy metals in natural environments.

Figure Captions

Figure 1. The 2-D X-ray images for the same region of BC and mineral nano particle consortium obtained using absorption contrast mode **(a)** and phase contrast mode **(e)**. Cross-section views of the reconstructed 3-D tomography under each mode at different depths relative to the position of gold nano particle along Z-axis as a reference. **(b)** and (**f**) are sections extracted at the position of the gold particle. **(c)** and **(g)** are sections extracted at 800 nm above the gold particle. **(d)** and **(h)** are sections extracted at 800 nm below the gold particle. The scale bar is 5 μm.

Figure 2. Three-directional orthogonal sections of lab-made BC and mineral nano particle consortium. The upper row sections are extracted from absorption contrast tomography **(a, b, c)**, and the lower row sections are extracted from phase contrast tomography **(d, e, f),** specifically (**a**) and (**d**) are for XY plane, (**b**) and (**e**) are for YZ plane, and (**c**) and (**f**) are for XZ plane. The scale bar is 5 μm.

Figure 3. 3-D tomography illustration of lab-made BC and mineral nano particle consortium observed at -45° (**a**, **d**), 0° (**b**, **e**), and +45° (**c**, **f**) azimuthal viewing angles under absorption contrast (**a**, **b**, **c**) and phase contrast mode (**d**, **e**, **f**). The scale bar is 5 μm.

Figure 4. Three-directional orthogonal sections of high mountain mineral-bearing OC from absorption contrast tomography (**a** for XY plane, **b** for XZ plane, and **c** for YZ plane). . The scale bar is 5 μm. Minerals mainly present two types of textures, subhedral particles and anhedral nano-aggregates. The lower row images highlight the free surface of specimen (red line in **d**), the boundary of OC (green dotted-line in **e**), and the subhedral mineral particles (pink arrow in **e** and **f**)

Figure 5. The X-ray diffraction pattern of minerals within OC particles from high mountain soil. Highly reactive Fe oxyhydroxides are identified and denoted with lines of different colors: ferrihydrite (ICDD 01-073-8408, orange), goethite (ICDD 01-073-6522, blue), and lepidocrocite (ICDD 00-044-1415, green). Q stands for Quartz (ICDD 00-033-1161). Details are included in Table S1.

Figure 6. Elementary mapping by SEM-EDS for mineral-bearing OC from high mountain soil. Left: SEM backscattering image (The bright spots inside are gold nano particles for coating). Right: Elemental mapping of C, O, Fe and Al. Scale bars are 20 µm.

Figure 7. The FTIR spectra for the chemistry of organo-mineral association. The aged OC is highly aromatic (1596 and 1386 cm^{-1}), and highly reactive with obvious carboxyl functional group (1706 cm^{-1}). The broad bands point to possible significant degree of association between OC and minerals. Some minor bands near 1274, 1062, 1024, and 989 cm^{-1} indicate the lignin-derived nature of OC. Those bands near 476, 534, 798, 910 and 1025 cm^{-1} have similar characteristics of soil inorganic/mineral matrix. More details are included in Table S2.

References

Alexandre, A., Basile-Doelsch, I., Delhaye, T., Borshneck, D., Mazur, J. C., Reyerson, P., and Santos, G. M.: New highlights of phytolith structure and occluded carbon location: 3-D X-ray microscopy and NanoSIMS results, Biogeosciences, 12, 863-873, 2015.

Baldock, J. A. and Skjemstad, J. O.: Role of the soil matrix and minerals in protecting natural organic materials against biological attack, Org. Geochem., 31, 697-710, 2000.

Bond, T. C., Doherty, S. J., Fahey, D. W., Forster, P. M., Berntsen, T., DeAngelo, B. J., Flanner, M. G., Ghan, S., Karcher, B., Koch, D., Kinne, S., Kondo, Y., Quinn, P. K., Sarofim, M. C., Schultz, M. G., Schulz, M., Venkataraman, C., Zhang, H., Zhang, S., Bellouin, N., Guttikunda, S. K., Hopke, P. K., Jacobson, M. Z., Kaiser, J. W., Klimont, Z., Lohmann, U., Schwarz, J. P., Shindell, D., Storelvmo, T., Warren, S. G., and Zender, C. S.: Bounding the role of black carbon in the climate system: A scientific assessment, J. Geophys. Res-Atmos., 118, 5380-5552, 2013.

Bousige, C., Ghimbeu, C. M., Vix-Guterl, C., Pomerantz, A. E., Suleimenova, A., Vaughan, G., Garbarino, G., Feygenson, M., Wildgruber, C., Ulm, F.-J., Pellenq, R.

J. M., and Coasne, B.: Realistic molecular model of kerogen's nanostructure, Nature Materials, 15, 576, 2016.

Chen, C., Dynes, J. J., Wang, J., Karunakaran, C., and Sparks, D. L.: Soft X-ray Spectromicroscopy Study of Mineral-Organic Matter Associations in Pasture Soil Clay Fractions, Environ. Sci. Technol., 48, 6678-6686, 2014a.

Chen, C. P., Cheng, C. H., Huang, Y. H., Chen, C. T., Lai, C. M., Menyailo, O. V., Fan, L. J., and Yang, Y. W.: Converting leguminous green manure into biochar: changes in chemical composition and C and N mineralization, Geoderma, 232, 581-588, 2014b.

Chen, K.-Y., Chen, T.-Y., Chan, Y.-T., Cheng, C.-Y., Tzou, Y.-M., Liu, Y.-T., and Teah, H.-Y.: Stabilization of Natural Organic Matter by Short-Range-Order Iron Hydroxides, Environ. Sci. Technol., 50, 12612-12620, 2016.

Chorover, J. and Amistadi, M. K.: Reaction of forest floor organic matter at goethite, birnessite and smectite surfaces, Geochim. Cosmochim. Acta, 65, 95-109, 2001.

Cornell, R. M. and Schwertmann, U.: The Iron Oxides: Structure, Properties, Reactions, Occurrences and Uses, Wiley, 2006.

Cusack, D. F., Chadwick, O. A., Hockaday, W. C., and Vitousek, P. M.: Mineralogical controls on soil black carbon preservation, Global Biogeochem. Cy., 26, 2019, 2012.

Eusterhues, K., Rennert, T., Knicker, H., Kögel-Knabner, I., Totsche, K. U., and Schwertmann, U.: Fractionation of Organic Matter Due to Reaction with Ferrihydrite: Coprecipitation versus Adsorption, Environ. Sci. Technol., 45, 527-533, 2011.

Eusterhues, K., Rumpel, C., and Kögel-Knabner, I.: Organo-mineral associations in sandy acid forest soils: importance of specific surface area, iron oxides and micropores, Eur. J. Soil Sci., 56, 753-763, 2005.

Eusterhues, K., Wagner, F. E., Häusler, W., Hanzlik, M., Knicker, H., Totsche, K. U., Kögel-Knabner, I., and Schwertmann, U.: Characterization of Ferrihydrite-Soil Organic Matter Coprecipitates by X-ray Diffraction and Mössbauer Spectroscopy, Environ. Sci. Technol., 42, 7891-7897, 2008.

Gu, B. H., Schmitt, J., Chen, Z. H., Liang, L. Y., and Mccarthy, J. F.: Adsorption and Desorption of Natural Organic-Matter on Iron-Oxide - Mechanisms and Models, Environ. Sci. Technol., 28, 38-46, 1994.

Hall, S. J., Silver, W. L., Timokhin, V. I., and Hammel, K. E.: Iron addition to soil specifically stabilized lignin, Soil Biol. Biochem., 98, 95-98, 2016.

Jeffery, S., Bezemer, T. M., Cornelissen, G., Kuyper, T. W., Lehmann, J., Mommer, L., Sohi, S. P., van de Voorde, T. F. J., Wardle, D. A., and van Groenigen, J. W.: The way forward in biochar research: targeting trade-offs between the potential wins, GCB. Bioenergy, 7, 1-13, 2015.

Kaiser, K., Eusterhues, K., Rumpel, C., Guggenberger, G., and Kogel-Knabner, I.: Stabilization of organic matter by soil minerals - investigations of density and particle-size fractions from two acid forest soils, J. Plant Nutr. Soil Sci., 165, 451-459, 2002.

Kaiser, K. and Guggenberger, G.: Sorptive stabilization of organic matter by microporous goethite: sorption into small pores vs. surface complexation, Eur. J. Soil Sci., 58, 45-59, 2007.

Kiem, R. and Kogel-Knabner, I.: Refractory organic carbon in particle-size fractions of arable soils II: organic carbon in relation to mineral surface area and iron oxides in fractions < 6 mu m, Org. Geochem., 33, 1699-1713, 2002.

Kinyangi, J., Solomon, D., Liang, B., Lerotic, M., Wirick, S., and Lehmann, J.: Nanoscale Biogeocomplexity of the Organomineral Assemblage in Soil, Soil Sci. Soc. Am. J., 70, 1708-1718, 2006.

Kleber, M., Sollins, P., and Sutton, R.: A conceptual model of organo-mineral interactions in soils: self-assembly of organic molecular fragments into zonal structures on mineral surfaces, Biogeochemistry, 85, 9-24, 2007.

Kuhlbusch, T. A. J.: Black carbon and the carbon cycle, Science, 280, 1903-1904, 1998.

Kuo, C.-H., Chu, Y.-T., Song, Y.-F., and Huang, M. H.: Cu2O Nanocrystal-Templated Growth of Cu2S Nanocages with Encapsulated Au Nanoparticles and In-Situ Transmission X-ray Microscopy Study, Adv. Funct. Mater., 21, 792-797, 2011.

Lehmann, J., Kinyangi, J., and Solomon, D.: Organic matter stabilization in soil microaggregates: implications from spatial heterogeneity of organic carbon contents and carbon forms, Biogeochemistry, 85, 45-57, 2007.

Lehmann, J., Solomon, D., Kinyangi, J., Dathe, L., Wirick, S., and Jacobsen, C.: Spatial complexity of soil organic matter forms at nanometre scales, Nat. Geosci., 1, 238-242, 2008.

Liang, B., Lehmann, J., Solomon, D., Kinyangi, J., Grossman, J., O'Neill, B., Skjemstad, J. O., Thies, J., Luizao, F. J., Petersen, J., and Neves, E. G.: Black Carbon increases cation exchange capacity in soils, Soil Sci. Soc. Am. J., 70, 1719-1730, 2006.

Liang, B., Lehmann, J., Solomon, D., Sohi, S., Thies, J. E., Skjemstad, J. O., Luizão, F. J., Engelhard, M. H., Neves, E. G., and Wirick, S.: Stability of biomass-derived black carbon in soils, Geochim. Cosmochim. Acta, 72, 6069-6078, 2008.

Mikutta, R., Kleber, M., and Jahn, R.: Poorly crystalline minerals protect organic carbon in clay subfractions from acid subsoil horizons, Geoderma, 128, 106-115, 2005.

Mikutta, R., Kleber, M., Torn, M. S., and Jahn, R.: Stabilization of Soil Organic Matter: Association with Minerals or Chemical Recalcitrance?, Biogeochemistry, 77, 25-56, 2006.

Mikutta, R., Mikutta, C., Kalbitz, K., Scheel, T., Kaiser, K., and Jahn, R.: Biodegradation of forest floor organic matter bound to minerals via different binding mechanisms, Geochim. Cosmochim. Acta, 71, 2569-2590, 2007.

Özçimen, D. and Ersoy-Meriçboyu, A.: Characterization of biochar and bio-oil samples obtained from carbonization of various biomass materials, Renew. Energy, 35, 1319-1324, 2010.

Rasmussen, C., Torn, M. S., and Southard, R. J.: Mineral assemblage and aggregates control carbon dynamics in a California conifer forest, Soil Sci. Soc. Am. J., 69, 1711-1721, 2005.

Rawal, A., Joseph, S. D., Hook, J. M., Chia, C. H., Munroe, P. R., Donne, S., Lin, Y., Phelan, D., Mitchell, D. R. G., Pace, B., Horvat, J., and Webber, J. B. W.: Mineral–

Biochar Composites: Molecular Structure and Porosity, Environ. Sci. Technol., 50, 7706-7714, 2016.

Schmidt, M. W. I.: Biogeochemistry: Carbon budget in the black, Nature, 427, 305-307, 2004.

Sharma, R. K., Wooten, J. B., Baliga, V. L., Lin, X., Geoffrey Chan, W., and Hajaligol, M. R.: Characterization of chars from pyrolysis of lignin, Fuel, 83, 1469-1482, 2004.

Sollins, P., Kramer, M. G., Swanston, C., Lajtha, K., Filley, T., Aufdenkampe, A. K., Wagai, R., and Bowden, R. D.: Sequential density fractionation across soils of contrasting mineralogy: evidence for both microbial- and mineral-controlled soil organic matter stabilization, Biogeochemistry, 96, 209-231, 2009.

Solomon, D., Lehmann, J., Harden, J., Wang, J., Kinyangi, J., Heymann, K., Karunakaran, C., Lu, Y., Wirick, S., and Jacobsen, C.: Micro- and nano-environments of carbon sequestration: Multi-element STXM–NEXAFS spectromicroscopy assessment of microbial carbon and mineral associations, Chem. Geol., 329, 53-73, 2012.

Sposito, G.: The Chemistry of Soils, Oxford University Press, 1989.

Torn, M. S., Trumbore, S. E., Chadwick, O. A., Vitousek, P. M., and Hendricks, D. M.: Mineral control of soil organic carbon storage and turnover, Nature, 389, 170-173, 1997.

Vogel, C., Mueller, C. W., Hoschen, C., Buegger, F., Heister, K., Schulz, S., Schloter, M., and Kogel-Knabner, I.: Submicron structures provide preferential spots for carbon and nitrogen sequestration in soils, Nat. Commun., 5, 2947, 2014.

Wang, C.-C., Song, Y.-F., Song, S.-R., Ji, Q., Chiang, C.-C., Meng, Q., Li, H., Hsiao, K., Lu, Y.-C., Shew, B.-Y., Huang, T., and Reisz, R. R.: Evolution and Function of Dinosaur Teeth at Ultramicrostructural Level Revealed Using Synchrotron Transmission X-ray Microscopy, Sci. Rep., 5, 15202, 2015.

Zbik, M. S., Frost, R. L., Song, Y. F., Chen, Y. M., and Chen, J. H.: Transmission X-ray microscopy reveals the clay aggregate discrete structure in aqueous environment, J. Colloid Interf. Sci., 319, 457-461, 2008.
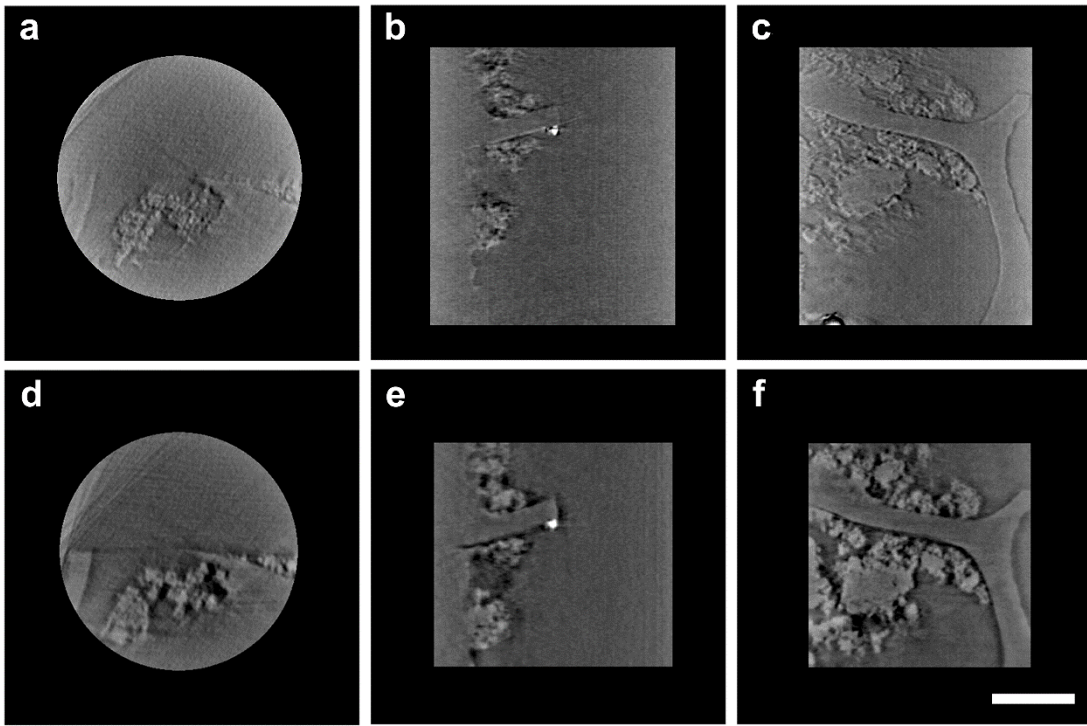
Zhao, Q., Poulson, S. R., Obrist, D., Sumaila, S., Dynes, J. J., McBeth, J. M., and Yang, Y.: Iron-bound organic carbon in forest soils: quantification and characterization, Biogeosciences, 13, 4777-4788, 2016.
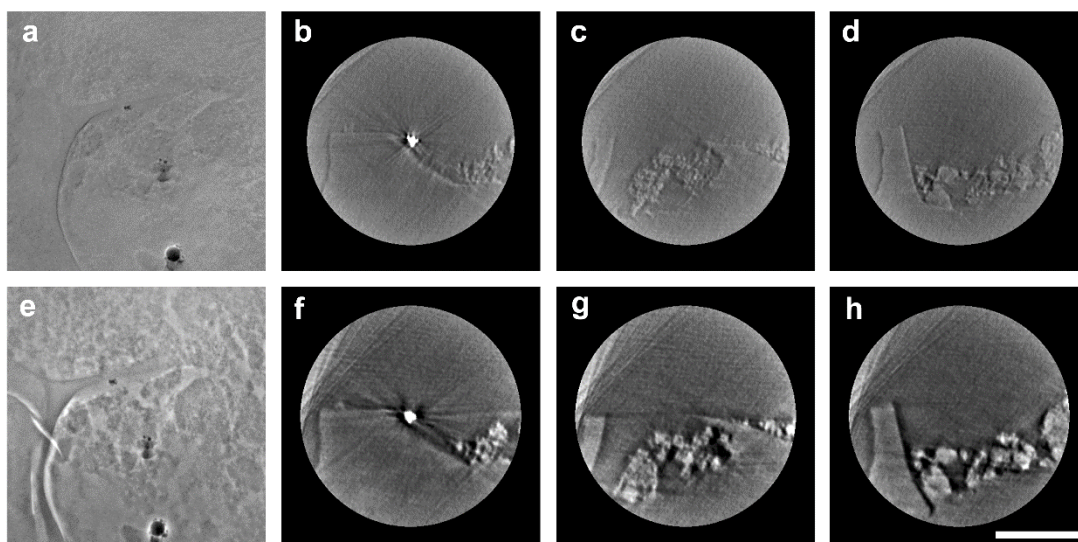
Figure 1.

Figure 2.

Figure 3.
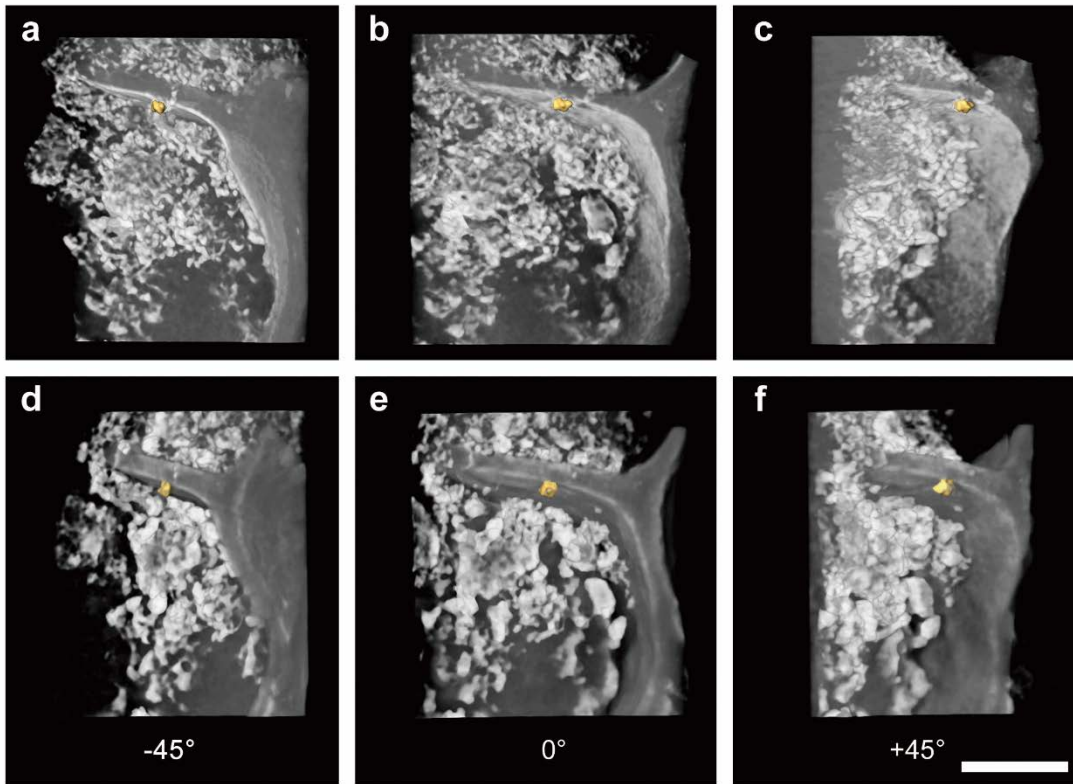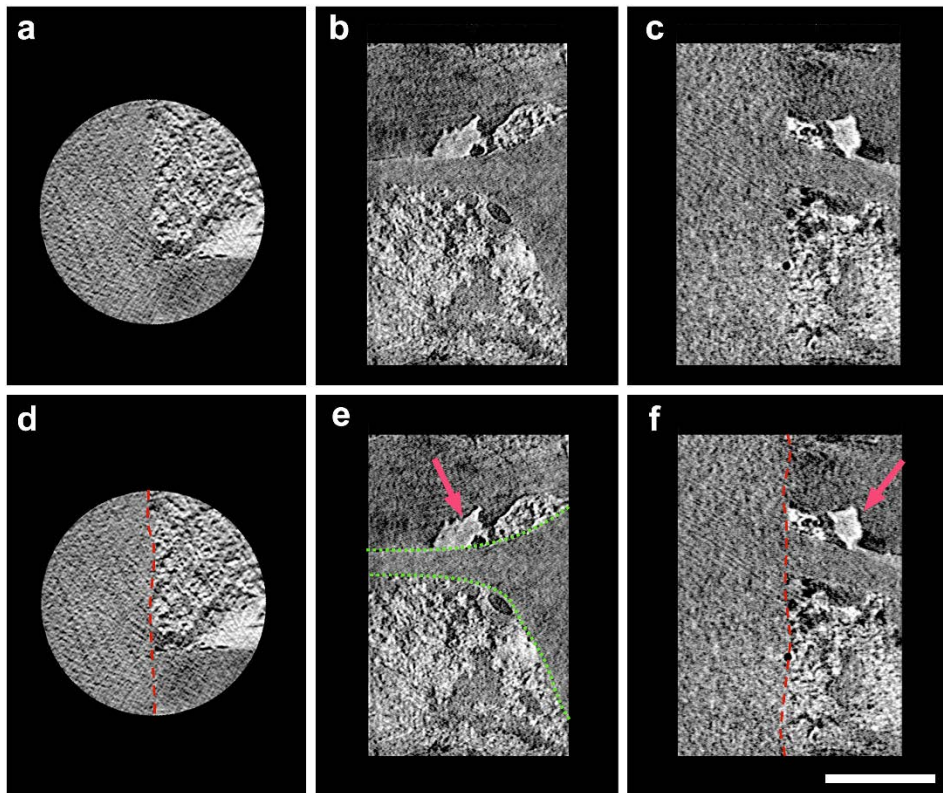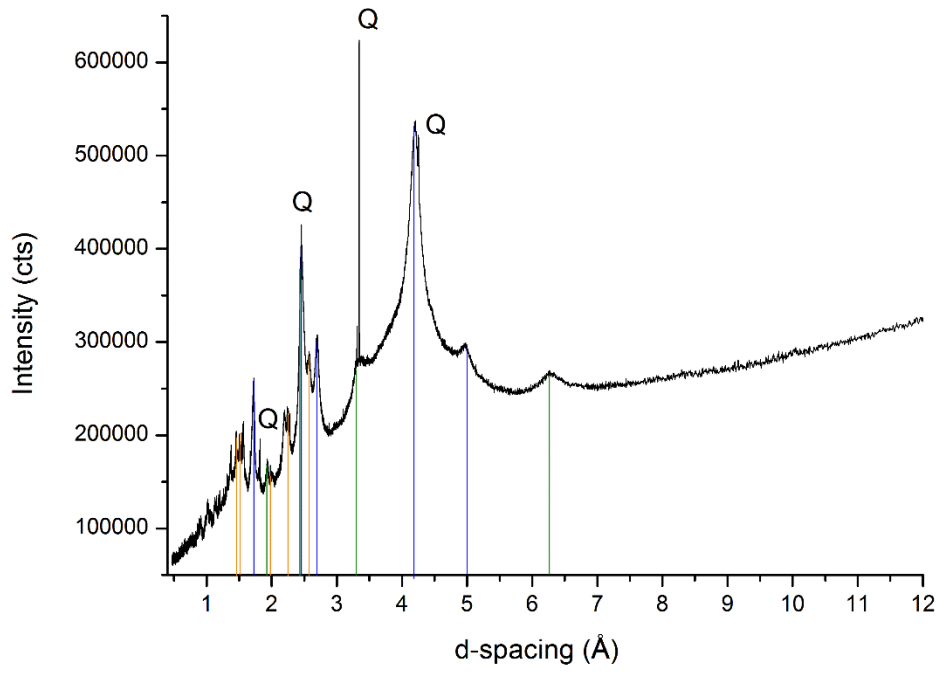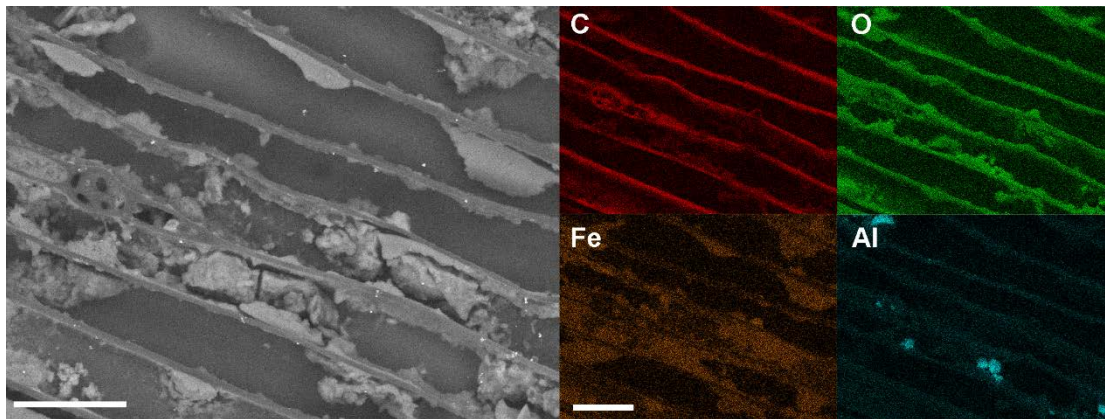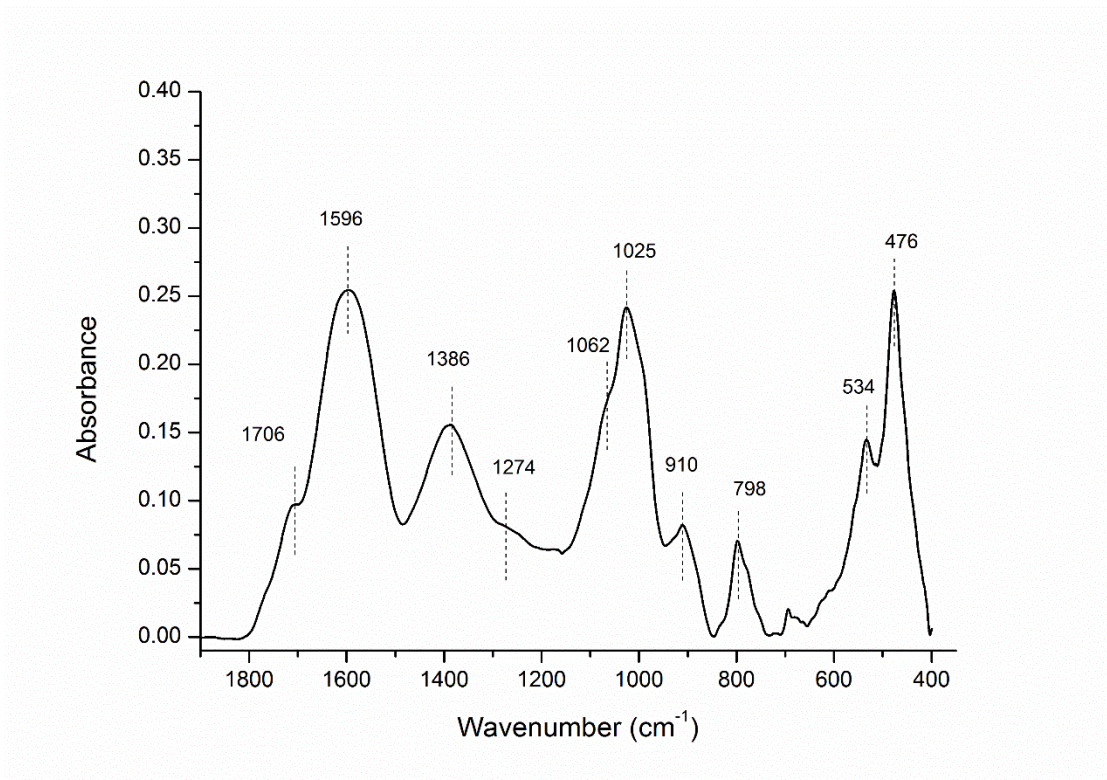
1

2

3 **Figure 4**.

1

2 **Figure 5**.

3

4

5

6 **Figure 6**.

1

2   **Figure 7**.

3